Phototautomerism in Uracil: A Quantum Chemical Investigation

M. K. Shukla and Jerzy Leszczynski*

Computational Center for Molecular Structure and Interactions, Department of Chemistry, Jackson State University, 1400 J. R. Lynch Street, Jackson, Mississippi 39217

Received: April 11, 2002; In Final Form: June 20, 2002

A detailed study of the molecular geometry and electronic spectra of uracil tautomers, anions, and their hydrated complexes was performed. The geometries were optimized both in the ground and lowest singlet excited states without any symmetry restriction. Ground-state geometries were optimized at the Hartree−Fock level of theory, while the excited states were generated by employing the configuration interaction technique involving singly excited configurations (CIS method). This was followed by excited-state geometry optimization. The nature of the corresponding potential energy surfaces was ascertained via an harmonic vibration frequency analysis. All geometries were found to be minima at their corresponding potential energy surfaces. The 6-311G-(d,p) basis set was used for neutral species, and the 6-311++G(d,p) basis set was used for anionic structures. It has been found that, in the gas phase and in aqueous solution at neutral pH, a normal uracil tautomer will phototautomerize to its monoenol tautomer, the fluorescence of which would be appreciably red-shifted compared to the normal fluorescence. At appreciable alkaline pH in aqueous solution, uracil would coexist as a neutral and monoanionic form obtained by deprotonation of the N1H site. While ground-state geometries are found to be planar, the corresponding excited-state geometries were predicted to be highly nonplanar.

1. Introduction

Two pyrimidine bases of nucleic acid, namely, uracil and thymine, differ with respect to each other only in the substitution of a methyl group at the C5 position in the latter. This causes appreciable modification of the photophysical properties, but electronic spectral properties are generally similar.[1] Thymine is photophysically most active among pyrimidines in view of photodimerization, while uracil is more stable.[1] A theoretical study of these compounds in the gas phase have suggested that while thymine is stable in the lowest singlet $\pi\pi^*$ excited state although its geometry is highly distorted, the corresponding state of uracil is dissociative due to the distortion of the C5C6 bond.[2] There are no direct experimental methods to determine the excited-state geometry of such a complex molecular system; however, the supersonic jet-cooled spectroscopic[3] and resonance Raman studies[4] have indicated the nonplanar excited-state geometries. Different theoretical[5] and experimental[6] investigations of uracil have been aimed at obtaining insight into the physical, chemical, and biological properties of the molecule. It is generally believed that uracil and thymine in the gas phase as well as in aqueous solution mainly exist in the diketo form. However, the existence of a small amount of the enol form of these compounds has also been indicated. Hauswirth and Daniels[7] have explained the observed deviation in the excitation spectrum of thymine from the corresponding absorption spectrum in terms of the possibility of emission from the enol tautomer. On the other hand, Vigny and Duquesne[8] observed that both the absorption and fluorescence excitation spectra of thymine are congruous. Suwaiyan et al.[9] have suggested the existence of a small amount of the enol tautomer in an aqueous solution of 5-chlorouracil at room temperature. The existence of keto−enol tautomerism in uracil, thymine, and their derivatives has also been suggested in supersonic jet-cooled spectroscopic studies.[10,11] However, Brady et al.[3] have shown that the observed sharp features in the excitation spectra of Fuji et al.[10,11] are due to the formation of some impurity produced in the oven. Recently, Morsy et al.[12] have performed detailed spectroscopic studies of the aqueous solution of thymine at different levels of pH. These authors[12] have found that the fluorescence peak for an aqueous solution of thymine at a neutral pH lies near 325 nm when excited in the range of 260−270 nm. A much stronger fluorescence band with a peak near 405 nm is observed with the excitation of the sample at 295 or 300 nm.[12] These observations have been explained in terms of the keto−enol tautomerism; the fluorescence peak near 325 nm is explained due to the emission from the keto tautomer, while the 405 nm fluorescence has been attributed to emission from the enol form of thymine which absorbs the longer wavelength region.[12] The concentration of the enol form is suggested to be about 2%.[12] The coexistence of neutral and protonated forms at a pH below 3 and that of neutral and deprotonated forms at a pH above 8 has also been suggested in an aqueous thymine solution.[12]

Hydration plays a very important role in biological systems. Different experimental investigations suggest that DNA is heavily hydrated and that such hydration plays an important role in base stacking and helix stabilization.[13,14] Studies of interactions of uracil and its analogues with several water molecules were also carried out by several authors employing different methods.[15,16] These studies are focused on the relative stabilities of different possible tautomers in the gas phase and under hydration, on the modes of interaction of water molecules, on the effects on the vibrational frequencies of the molecules, and on the planarity of the molecules. Shishkin et al.[16a] have studied the hydration of uracil and thymine with 11 water molecules at the B3LYP level employing the 6-31G(d) basis set and have found that the structures of the water cage around molecules are entirely different from each other. The presence of a methyl group in thymine induces strong nonplanarity in

* Corresponding author.

10.1021/jp0209650 CCC: $22.00
Published on Web 08/21/2002

TABLE 1: Relative Energy (ΔE, kJ/mol) of Different Tautomers of Uracil and Their Complexes with Three Water Molecules at the HF/6-311G(d,p) Level[a]

	isolated form		hydrated form		earlier results[b]	
tautomer	HF	MP4//HF[c]	HF	MP4//HF[c]	DFT[d]	MP4//HF[e]
neutral tautomers						
uracil	0.0	0.0	0.0	0.0	0.0	0.0
enol	54.5	51.8	48.6	39.5	53.5	54.0
U-O2H1	48.5	47.0	38.1	33.2	46.4	48.1
U-O4H3	57.7	53.1	36.9	27.5	50.0	-
U-O2H3	86.4	83.7	64.9	57.5	81.8	-
anions						
U-N1$^-$	0.0		0.0			
U-N3$^-$	61.7		36.7			

[a] Relative total energy for anions obtained at the HF/6-311++G(d,p) level is also given. [b] Corresponds to isolated uracil. [c] At the MP4(SDTQ)/6-31G(d,p)//HF/6-311G(d,p) level, present study. [d] At the B3LYP/6-31+G(d,p) level, see ref 5g. [e] At the MP4(SDTQ)/6-31G(d,p)//HF/6-31G(d,p) level, see ref 5c.

the hydrated shell. Furthermore, the existence of C−H···O hydrogen bonds between the water molecules and the hydrophobic part of the nucleobases is also revealed. The predicted geometrical deformations were explained by taking into account the contribution of a zwitterionic dihydroxy resonance form into the total structure of the molecules. In another related study, the pyrimidine ring of nucleic acid bases were shown to be very flexible, and at any given moment, only about 50% of the molecule possesses a planar structure in the ground state.[16b]

To the best of our knowledge, there are no experimental and theoretical studies pertaining to interactions of water molecules with uracil in excited states. However, studies of other systems such as 7-azaindole and water complex have suggested that the mode of interaction is entirely different in the n−π* state compared to the ground and $\pi-\pi$* excited states.[17] In the ground and $\pi-\pi$* excited states, the 7-azaindole acts both as a hydrogen bond donor and acceptor, while in the n−π* excited state it acts only as a hydrogen bond donor.[17] We have recently found that the nucleic acid base pairs are destabilized in the n−π* excited states.[18] In an experimental study of indole−water interactions, the orientation of the water molecule was found to change consequentially to excitation; the hydrogen bond distance was also found to decrease.[19] A recent experimental study of hydrated clusters of adenine in a supersonic molecular beam shows weakening in the hydrogen bonding and the subsequent fragmentation of the adenine monomer hydrated clusters in the n−π* excited state of adenine.[20] In the present work we have undertaken ground- and excited-state geometry optimization calculations of uracil tautomers, anions, and their complexes with water molecules with the aim of investigating the keto−enol tautomerism of uracil in the ground and excited states and to examine if the observed fragmentation of the hydrated adenine cluster in the nπ* excited state is also valid for uracil.

2. Computational Details

The ground-state geometries of all considered species were optimized using the ab initio restricted Hartree−Fock method. The excited states were generated using the configuration interaction considering single electron excitations (CIS) from filled to unfilled molecular orbitals using the optimized ground-state geometry, and this was followed by geometry optimizations in different excited states. The standard 6-311G(d,p) basis set was used for neutral species, while the 6-311++G(d,p) basis set was used for anionic species. The nature of the corresponding ground- and excited-state optimized potential energy surfaces (PESs) was analyzed by vibrational frequency calculations and was found to be minima on the respective PES. In the CIS calculation[21] all of the occupied and unoccupied molecular orbitals were considered using the option CIS=FULL. The single point energy calculations were also performed at the MP4(SDTQ)/6-31G(d,p) level using ground-state HF optimized geometries. All calculations were performed using the Gaussian 94 program.[22]

It is well-known that CIS computed transition energies are much larger than the corresponding experimental excitation energies, and some scaling factors are needed to bring the computed excitation energies closer to the experimental values.[23] Such scaling is not uncommon in computational chemistry including those of high levels of quantum chemical methods. Different scaling factors, depending upon the level of theories and basis sets, are frequently used for zero-point vibrational energy corrections and vibrational frequency analyses.[24] The CIS method is considered the zero-order approximation to study the excited-state potential energy surface and is the HF analogue for excited-state calculations.[21] Despite the well-known deficiency of the CIS method, it has been successfully applied to studies of excited-state properties including the geometries of varieties of molecules.[23,25]

3. Results and Discussion

3.1. Ground-State Relative Stability. The ground-state relative total energy of the keto and different enol tautomers of uracil (U) are presented in Table 1, while the atomic numbering scheme for uracil is shown in Figure 1a. It should be noted that our aim is not to emphasize the ground-state properties as has already been previously discussed by other investigators;[5] rather we will discuss excited-state properties in detail. The discussion of the ground-state properties will be limited only to the relative total energies and their comparison with earlier theoretical results performed with electron correlated methods. The relative stability of tautomers in the gas phase follows the order:

U-keto > U-O2H1 > U-enol > U-O4H3 > U-O2H3

This stability order and the value of relative energy (Table 1) is in agreement with the previously computed results at the B3LYP/6-31+G(d,p) level[5g] and other single point electron correlated levels for which the HF geometry was used.[5c] Here the nomenclature of different tautomers are such that U-enol represents the dienol tautomer, while U-OmHn represents the mono enol tautomer in which the Hn hydrogen atom attached to the Nn site of the keto form of the uracil ring is attached to the Om carbonyl oxygen. We have considered the effect of aqueous hydration using the super molecular approach in which three water molecules were attached to the uracil tautomers.

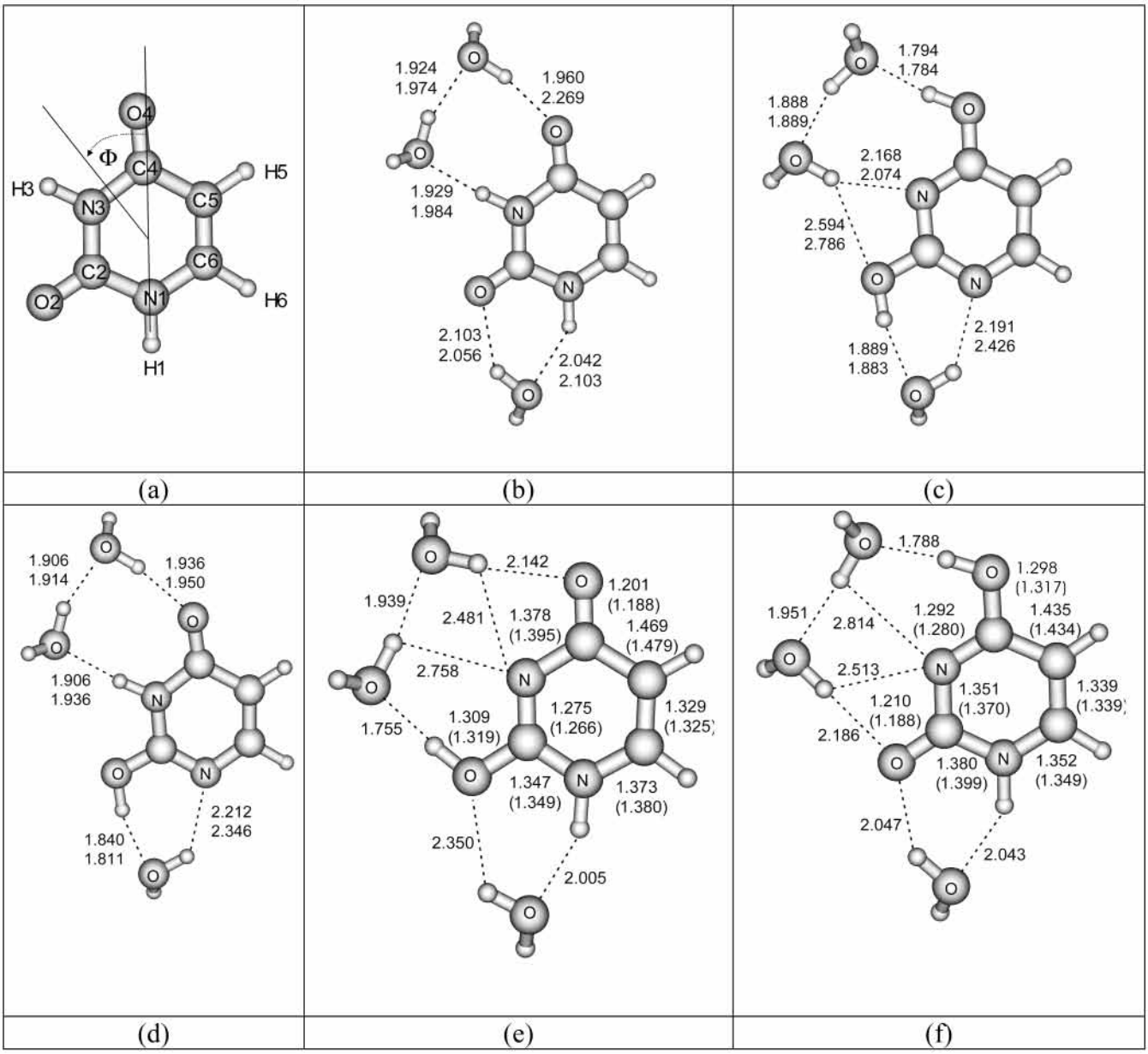

Figure 1. Structure and atomic numbering schemes of uracil (keto) in (a). Hydrogen bond lengths of hydrated uracil (keto) tautomer in the ground state (top indices) and in the lowest singlet nπ^* state (bottom indices) in (b), hydrogen bond lengths of hydrated enol tautomer in the ground state (top indices) and in the lowest singlet $\pi\pi^*$ state (bottom indices) in (c), hydrogen bond lengths of hydrated U-O2H1 tautomer in the ground state (top indices) and in the lowest singlet $\pi\pi^*$ state (bottom indices) in (d), hydrated complex of U-O2H3 tautomer in the ground state in (e), and hydrated complex of U-O4H3 tautomer in the ground state in (f). The upper and lower indices (in parentheses) in e and f correspond to the hydrated and unhydrated forms in the ground state. Φ shows the transition moment direction according to Tinoco−DeVoe convention.

Chahinian et al.[26] have shown experimentally using Overhauser spectroscopy that the first solvation shell of uracil indeed includes three water molecules. These authors have suggested that water binding with uracil will be a cyclic trihydrated complex in which each of the water molecules will be bonded between the NH and C═O groups. However, the present computation suggests that water will not be bonded between the N3H and C2O groups; rather one water molecule will be bonded between the N1H and C2O groups, while two water molecules will be bonded between the N3H and C4O groups (Figure 1b). The optimized structures of complexes of three water molecules with uracil tautomers are shown in Figure 1. The relative stability of different tautomers is changed after water complexation and can be given as follows:

U-keto > U-O4H3 > U-O2H1 > U-enol > U-O2H3

Here it should be noted that while in the gas-phase U-O2H1 is about 9.2 kJ/mol more stable than the U-O4H3 tautomer, after complexation with three water molecules, it is about 1.2 kJ/mol less stable (Table 1). These findings are also validated from the single point calculation at the MP4(SDTQ)/6-31G(d,p) level using HF/6-311G(d,p) optimized geometries, though energy difference for hydrated species is slightly higher (Table 1). Thus uracil will be present mainly in the normal keto form in the gas phase and in an aqueous environment.

Among anions, the anion (U-N1$^-$) obtained by the deprotonation of the N1 site is about 61.7 kJ/mol more stable than the anion (U-N3$^-$) obtained by the deprotonation of the N3 site of uracil (Table 1). However, after complexation with three water molecules (Figure 2), the energy difference between two anions is found to be about 36.7 kJ/mol (Table 2). The U-N1$^-$ anion was also found to be most stable at the B3LYP/6-31+G(d,p)

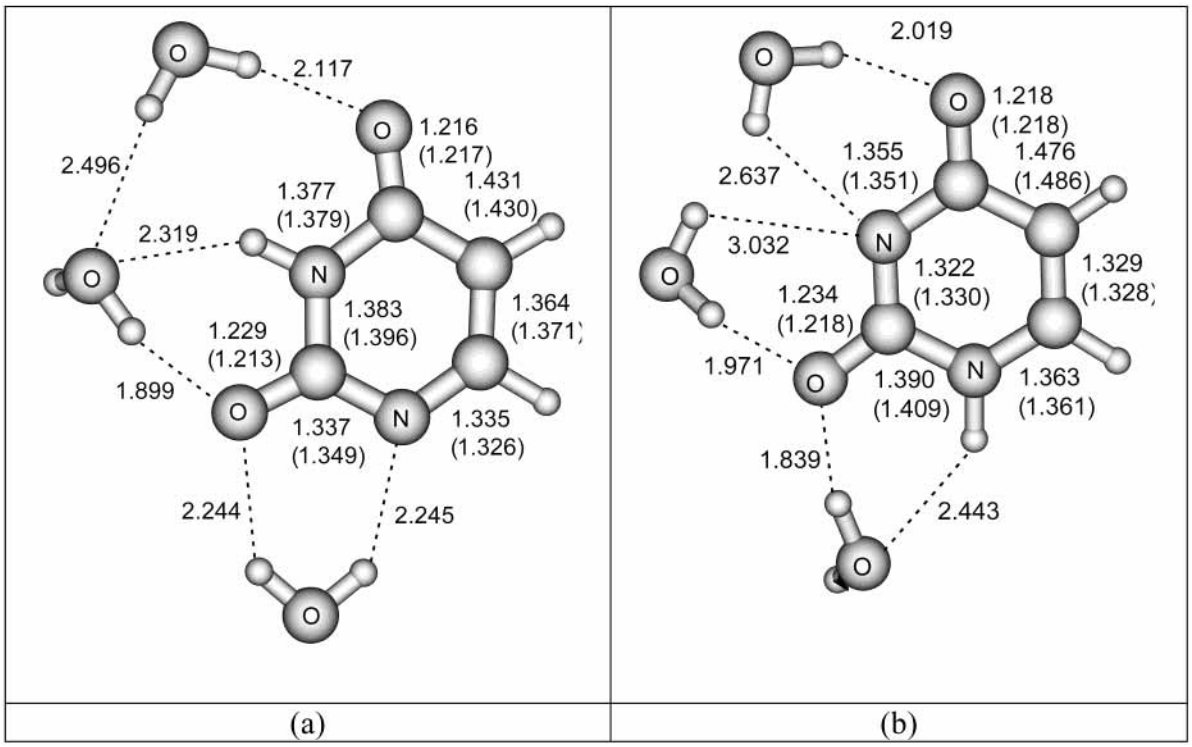

Figure 2. Hydrated complexes of uracil anions U-N1$^-$ in (a) and U-N3$^-$ in (b). The upper and lower indices correspond to the hydrated and unhydrated parameters.

level of theory.[5g] The predicted stability of the U-N1− anion is in accordance with the computational predictions that the N1H bond is more acidic than the N3H bond in uracil.[5g]

3.2. Vertical Transitions. The CIS computed transition energies of uracil in the gas phase and after hydration (with three water molecules) are shown in Table 2 along with the respective electronic spatial extent ($\langle R^2 \rangle$) values. For the sake of comparison, the scaled (scaling factor 0.72)[18] computed $\pi\pi^*$ and nπ^* transition energies along with selected experimental and CASSCF/CASPT2 transition energies are shown in Table 2. Electronic transitions are characterized by one of the $\pi\pi^*$, nπ^*, or $\pi\sigma^*$ types of transition. Further, the computed electronic spatial extent ($\langle R^2 \rangle$) values for the ground state and different $\pi\pi^*$ and nπ^* states (vertical) are almost the same, while values for the $\pi\sigma^*$ states (vertical) are slightly higher (Table 2). This suggests that the $\pi\pi^*$ and nπ^* transitions are valence type, while the $\pi\sigma^*$ transitions are contaminated by some Rydberg orbitals.[27] Among all nπ^* transitions, the first transition is localized at the C4O4 group, the second is localized at the C2O2 group, and the third is of the mixed type with contributions from both of the C4O4 and C2O2 groups. Assignments of these transitions are in agreement with the MRCI, RPA,[5e] and CASSCF/CASPT2 results.[28] Data shown in Table 2 suggest that after complexation with water molecules, the nπ^* transition energies are increased. Therefore, while in the gas phase (isolated molecules), the first vertical singlet excited state of uracil has nπ^* character; after complexation with water molecules, the $\pi\pi^*$ state lies lower. This change in the ordering of the excited state is in accordance with experimental observation in which in the gas phase or in an aprotic solvent uracil and thymine have the nπ^* state as the lowest singlet excited state, while in a protic solvent the $\pi\pi^*$ state is the lowest.[1a,29] The computed first nπ^* transition after complexation with water molecules has an energy of 6.79 eV; the corresponding scaled value is 4.89 eV (Table 2). There is sufficient experimental and theoretical evidence to believe that the existence of a nπ^* transition is near 250 nm (4.96 eV) of uracil in an aqueous medium, the relative position of which is solvent dependent.[1a,28,30] The computed second nπ^* transition in uracil is predicted near 5.8 eV (scaled value; Table 2). The existence of an nπ^* transition to be near 217 nm (5.71 eV) has been previously suggested in 1-methyluracil,[31] which is in good agreement with the CIS prediction. Data shown in Table 2 suggest that there is good correspondence between the CIS computed scaled $\pi\pi^*$ excitation energies and CASPT2 $\pi\pi^*$ excitation energies except that of the second transition.[28] Fairly good agreement is also found between the CIS computed (scaled) and experimentally observed transition energies of uracil (Table 2). The observed gas-phase transitions of uracil are in good agreement with the computed $\pi\pi^*$ transition except the second one for which the disagreement is a little bit higher (Table 2).[32a] In aqueous solution at a neutral pH, uracil shows absorption peaks near the 259 (4.79), the 202 (6.14), and the 181 nm (6.85 eV) regions.[32b] These transitions can be explained in terms of the computed $\pi\pi^*$ transitions of hydrated uracil near 4.85, 6.29, and 7.15 eV (Table 2). The CD spectra reveal the composite nature of the 205 nm region absorption band with peaks near 215 nm (5.77 eV) and 195 nm (6.36 eV).[30c] The composite nature of the 205 nm (6.05 eV) band observed in the CD spectra[30c] of uracil is also revealed by CIS computations, although splitting is slightly smaller (Table 2). Observed CD spectra of an aqueous solution of uridine and those of the aqueous absorption spectra of uracil can be easily explained in terms of the computed (scaled) vertical $\pi\pi^*$ transitions of hydrated uracil within an error of 0.2 eV except the second transition for which the error is a little bit higher. However, if one compares the computed transitions with the corresponding experimental range obtained in different experiments,[1a,28−33] the agreement is good (Table 2). The CIS computed transition moment direction for the first $\pi\pi^*$ transition is found to be −7° (−6° for hydrated species; Table 2). This prediction is in agreement with the experimental value of −9° by Vovrous and Clark for uracil.[31] For the second transition, Novros and Clark[31]

TABLE 2: Vertical Excitation Energies (ΔE, eV), Oscillator Strengths (f), Transition Moment Directions (Φ, deg), Dipole Moments (μ, D), and Electronic Spatial Extent ($\langle R^2 \rangle$, au) of Uracil Tautomers in the Gas Phase and after Hydration[a]

	gas phase				hydrated			CASPT2/CASSCF[b]	exptl[c]				
state	ΔE	f/Φ	$\langle R^2 \rangle$	μ	ΔE	f/Φ	$\langle R^2 \rangle$	$\Delta E^1/\Delta E^2/f/\Phi/\mu$	abs[1]	abs[2]	CD	crystal	expt range
uracil (keto)													
S_0			814	4.67			2738	−/−/−/−/4.44					
$S_1(n\pi^*)$	6.51	0.000	810	2.82	6.79	0.001	2735						
	(4.69)				(4.89)			4.54/4.78/−/−/3.4					
$S_2(\pi\pi^*)$	6.83	0.446	814	5.07	6.74	0.447	2738						
	(4.92)	−7			(4.85)	−6		5.00/6.88/0.19/− 7/6.3	5.08	4.79	4.73	4.51/−9	4.6−4.9
$S_3(\pi\sigma^*)$	7.85	0.002	834	2.49	8.19	0.008	2766						
$S_4(n\pi^*)$	7.98	0.000	809	5.10	8.11	0.000	2735						
	(5.75)				(5.84)			6.00/6.31/−/−/4.8					
$S_5(\pi\pi^*)$	8.89	0.123	814	3.48	8.73	0.140	2738						
	(6.40)	36			(6.29)	46		5.82/7.03/0.08/−29/2.4	6.05	6.14	5.77	5.82/59	5.8−6.1
$S_6(\pi\sigma^*)$	9.18	0.020	835	0.78									
$S_7(\pi\pi^*)$	9.29	0.386	814	4.99	9.12	0.439	2739						
	(6.69)	−66			(6.57)	−57		6.46/8.35/0.29/23/6.9	6.63		6.36		6.3−6.6
$S_8(n\pi^*)$	9.96[c]	0.006	820	7.06	9.97	0.009	2738						
	(7.17)				(7.18)			6.37/7.80/−/−/8.7					
$S_9(n\pi^*)$	9.98[c]	0.000	818	6.15									
$S_{10}(\pi\pi^*)$	10.0	0.322	814	2.43	9.93	0.251	2743						
	(7.2)	−14			(7.15)	−15		7.00/8.47/0.76/−42/3.7		6.85	7.00		6.8−7.0
enol													
S_0			812	1.30			2552						
$\pi\pi^*$	6.65	0.180	812	1.08	6.62	0.213	2552						
	(4.79)	−4			(4.77)	−5							
$n\pi^*$	7.04	0.007	812	1.61	7.30	0.006	2552						
	(5.07)				(5.26)								
$\pi\pi^*$	7.60	0.076	812	1.75	7.63	0.081	2552						
	(5.47)	−88			(5.49)	−74							
U-O2H1													
S_0			814	3.45			2684						
$\pi\pi^*$	6.36	0.316	815	3.09	6.40	0.342	2684						
	(4.58)	−27			(4.61)	−23							
$n\pi^*$	6.75	0.000	811	1.31	7.02	0.000	2682						
	(4.84)				(5.05)								
$\pi\pi^*$	8.25	0.276	815	3.43	8.12	0.281	2683						
	(5.94)	39			(5.85)	41							
U-O4H3													
S_0			812	5.19			2477						
$\pi\pi^*$	6.27	0.190	812	4.37	6.46	0.202	2478						
	(4.51)	26			(4.65)	23							
$n\pi^*$	7.08	0.002	812	2.39	7.26	0.002	2481						
	(5.10)				(5.23)								
$\pi\pi^*$	8.33	0.210	813	5.89	8.19	0.123	2477						
	(6.00)	−65			(5.90)	−77							
U-O2H3													
S_0			814	6.71			2460						
$n\pi^*$	6.04	0.000	811	3.45	6.42	0.000	2456						
	(4.35)				(4.62)								
$\pi\pi^*$	6.91	0.199	815	6.08	6.88	0.222	2461						
	(4.98)	−14			(4.95)	−12							
$\pi\pi^*$	8.11	0.403	814	6.71	8.02	0.331	2460						
	(5.84)	10			(5.77)	11							

[a] The scaled (scaling factor 0.72) excitation energies for the $\pi\pi^*$ and $n\pi^*$ states are given in parentheses. In the case of enol tautomers only vertical three singlet transition energies of $\pi\pi^*$ or $n\pi^*$ types are given. [b] ΔE^1 represents CASPT2 and ΔE^2 represents CASSCF transition energies, for the f values of $n\pi^*$ transitions; see original paper.[28] [c] Abs[1] represents absorption in the gas phase,[32a] Abs[2] represents absorption in aqueous medium,[32b] CD represents CD spectra in aqueous medium,[30c] crystal represents the transition energy/transition moment direction,[31] and expt. range represents the experimental range of transitions observed in different experiments.[1a,28−33] [d] Slightly contaminated with $\pi\sigma^*$ transition.

have suggested two transition moment directions, namely, −53° or +59°, and favor the latter as being consistent with the LD spectra of uracil.[33a] But Anex et al.[33b] have suggested −31°. Eaton and Lewis have estimated that polarization of the I and II bands are approximately perpendicular to each other.[33c] Holmen et al.[33d] have found an angle of 35° for the second transition of 1,3-dimethyluracil. Thus, our computed transition moment direction value of 36° (46° for hydrated species) for the second transition is in agreement with the predictions of Vovrous and Clark[31] and the predictions of Holmen et al.[33d]

The absorption spectrum of uracil in an aqueous medium at pH 14 shows a peak near 276 nm (4.49 eV) and a shoulder near the 230 nm (5.39 eV) region.[32b] Absorption spectrum of thymine at pH 12 shows a peak near 290 nm (4.28 eV) and a shoulder near 265 nm (4.68 eV).[12] The buildup of the peak near 290 nm starts with pH 9 in the form of a weak shoulder and increases progressively with an increase in the pH of the solution. It has been suggested that monoanions of thymine obtained by deprotonation of the N1 and N3 sites will be present in the solution at pH 12.[12] With uracil and thymine being different from each other only at the methyl substitution site at the C5 position, absorption and fluorescence peaks are revealed approximately at a similar region, although the main absorption peak in uracil is about 5 nm blue-shifted compared to the

TABLE 3: Low-Lying Vertical Singlet $\pi\pi^*$ and $n\pi^*$ Excitation Energies (ΔE, eV), Oscillator Strength (f), and Assignment of Uracil Anions in the Gas Phase and after Hydration[a]

	gas phase		hydrated form		exptl
state/assigmt	ΔE	f	ΔE	f	data[b]
U-N1$^-$					
$\pi\pi^*$	5.77	0.388	5.90	0.413	
	(4.15)		(4.25)		4.49
$\pi\pi^*$	6.08	0.035			
	(4.38)				
$\pi\pi^*$	7.01	0.143	7.44	0.118	
	(5.04)		(5.58)		5.39
$n\pi^*$	7.05	0.000	7.23	0.002	
	(5.08)		(5.21)		
U-N3$^-$					
$n\pi^*$	6.29	0.001	6.50	0.003	
	(4.53)		(4.68)		
$\pi\pi^*$	6.39	0.146	6.59	0.212	
	(4.60)		(4.74)		
$\pi\pi^*$	6.78	0.028			
	(4.88)				
$\pi\pi^*$	7.00	0.084	7.46	0.082	
	(5.04)		(5.37)		

[a] The scaled (scaling factor 0.72) excitation energies are given in parentheses. [b] See ref 32b.

corresponding peak of thymine.[1a,32] We hope that the nature of both molecules thymine and uracil would be generally similar at alkaline pH also. Vertical singlet $\pi\pi^*$ and $n\pi^*$ excitation energies of two anions of uracil (U-N1$^-$ and U-N3$^-$) in the gas phase and their hydrated forms are shown in Table 3. This table shows that in the gas phase the lowest singlet $\pi\pi^*$ excited state of the U-N3$^-$ anion is about 1.26 eV higher in energy than the corresponding state of the U-N1$^-$ anion, while for hydrated species this difference is 1.07 eV. As discussed previously, in the ground state the U-N3$^-$ anion is about 0.64 eV (61.7 kJ/mol) less stable than the U-N1$^-$ anion; the corresponding value for hydrated species is 0.38 eV (36.7 kJ/mol). These results suggest that U-N3$^-$ can neither be formed in the ground state nor in the excited state through phototautomerization. Table 3 shows that the U-N1$^-$ anion in the gas phase has a weak transition near 4.38 eV but is not observed in the hydrated form of the U-N1$^-$ anion. It appears that under hydration it would merge to the first $\pi\pi^*$ transition (Table 3). The 276 nm (4.49 eV) absorption peak and 230 nm (5.39 eV) absorption shoulder of aqueous solution of uracil[32b] obtained at pH 14 can be explained in terms of the computed lowest two singlet $\pi\pi^*$ excitations at 4.25 and 5.58 eV of the hydrated U-N1$^-$ anion (Table 3). The observed absorption peak of thymine[12] near 290 nm (4.28 eV) can also be explained in terms of the computed first $\pi\pi^*$ transition of the hydrated U-N1$^-$ anion (Table 3). However, the observed shoulder of thymine[12] near 265 nm (4.68 eV) cannot be explained in terms of the computed transitions of the U-N1$^-$ anionic species although the lowest singlet $\pi\pi^*$ transition of the U-N3$^-$ anion lies near the 4.6 eV (scaled value) region. As discussed earlier, it is unlikely that the U-N3$^-$ anion would be present in an aqueous medium or in the gas phase. However, this shoulder lies in the region of the main absorption band of the neutral species and can be explained easily in terms of the first $\pi\pi^*$ transition of the neutral species (Table 2). Thus, it appears that even at pH 12, some neutral forms of thymine are presentl and are contributing to the absorption peak near 265 nm, while strong peaks near 290 nm are due to an anion obtained from the deprotonation at the N1H site. Evidently, the fluorescence of thymine observed near 375 nm at pH 12 would originate from the relaxed lowest singlet $\pi\pi^*$ excited state of an anion obtained by deprotonation of the N1H site of the molecule.[12]

3.3. Dipole Moments. The computed gas-phase ground-state dipole moment of uracil (keto) is found to be 4.67 D (Table 2). The observed dipole moment for uracil using the microwave spectroscopic method[6e] is found to be 3.87 D, while in a dioxane solution[6f] it is 4.16 D. The computed dipole moment at the CASSCF/CASPT2 level[28] is 4.4 D. Therefore, our computed gas-phase dipole moment is closer to those observed in a dioxane solution.[6f] In going from the ground state to the first singlet $\pi\pi^*$ excited state of uracil, the computed dipole moment is increased (Table 2). The dipole moment of thymine is also found experimentally to increase consequentially to excitation.[34] The experimentally determined dipole moment for the first singlet $\pi\pi^*$ excited state of thymine is 5.3 D.[34] The predicted dipole moment is in agreement with the CIS computed gas-phase dipole moment of the lowest singlet $\pi\pi^*$ transition of uracil (Table 2).

3.4. Ground- and Excited-State Geometries. Ground- and excited-state optimized ring geometries of uracil tautomers and their hydrated complexes are presented in Table 4, while their structures along with hydrogen bond distances are shown in Figure 1. Although the ground-state geometries of uracil tautomers are planar in the gas phase and under hydration, the corresponding excited-state geometries are found to be appreciably nonplanar (Table 4). The ring geometry of the keto tautomer in the $n\pi^*$ state is slightly nonplanar; the C4O4 bond length is increased appreciably by about 0.1 Å and is lying appreciably away from the approximate ring plane. Such deformation is consistent with the fact that the excitation is localized at the C4O4 group. The ring geometry of the hydrated complex does not change much in the ground and $n\pi^*$ excited states compared to the corresponding geometry of the isolated form (Table 4). Hydrogen bonding parameters for hydrated uracil keto tautomers in the ground and $n\pi^*$ excited states shown in Figure 1b suggest that the hydrogen bond distance associated with the C4O4 group is only increased in the $n\pi^*$ excited state and that no fragmentation in the hydrogen bonded cluster is found. Therefore, the observed fragmentation in hydrated adenine is not found for the uracil keto tautomer in its lowest singlet $n\pi^*$ excited state.[20] Ring geometries for the ground and lowest singlet $\pi\pi^*$ excited state of the enol and U-O2H1 tautomers of uracil and their hydrated complexes are also shown in Table 3, while corresponding hydrogen bonded structures along with the hydrogen bond distances are shown in Figure 1. The ground-state ring geometries of these tautomers and their hydrated complexes are planar; the corresponding lowest singlet $\pi\pi^*$ excited-state geometries are appreciably nonplanar. In going from the ground state to the lowest singlet $\pi\pi^*$ excited state of the enol tautomer, the geometrical deformation is revealed mainly in the N1C6C5C4 portion of the ring; the N1C2N3C4 atoms are in one plane, while C5C6 atoms are appreciably out of plane and slightly twisted along the perpendicular direction of the C5C6 bond. Furthermore, the C5C6 bond length is appreciably increased by about 0.09 Å in the excited state; the N1C2 and N3C4 bond lengths are also increased by about 0.03 and 0.04 Å in this (excited) state (Table 4). Among bond angles, N1C6C5 is decreased by about 17° in the excited state. Hydration reveals little effect on the geometrical parameters both in the ground and excited states compared to the corresponding isolated geometries of the tautomer (Table 4). The hydrogen bond parameters shown in Figure 1c suggest that the hydrogen bond distances are generally not affected consequent to $\pi\pi^*$

TABLE 4: Ground- and Excited-State Optimized Bond Lengths (Å), Bond Angles (deg), and Dihedral Angles (deg) of Uracil Tautomers in the Gas Phase and after Hydration with Three Water Molecules Employing the 6-311G(d,p) Basis Set

	uracil (keto)				enol				U-O2H1			
	S_0		$S_1(n\pi^*)$		S_0		$S_1(\pi\pi^*)$		S_0		$S_1(\pi\pi^*)$	
	isolated	hydrated	isolated	hydrated	isolated	hydrated	isolated	hydrated	isolated	hydrated	isolated	hydrated
Bond Lengths												
C2N1	1.373	1.370	1.371	1.370	1.310	1.313	1.344	1.348	1.275	1.289	1.332	1.325
N3C2	1.370	1.366	1.367	1.357	1.320	1.324	1.300	1.311	1.343	1.342	1.363	1.347
C4N3	1.391	1.380	1.417	1.415	1.308	1.315	1.350	1.351	1.400	1.386	1.442	1.419
C5C4	1.463	1.458	1.465	1.467	1.397	1.405	1.380	1.392	1.451	1.444	1.432	1.424
C6N1	1.371	1.365	1.388	1.380	1.330	1.336	1.356	1.354	1.371	1.364	1.312	1.334
C6C5	1.328	1.331	1.326	1.328	1.368	1.361	1.458	1.458	1.341	1.343	1.438	1.451
O2C2	1.188	1.196	1.191	1.201	1.319	1.314	1.306	1.298	1.315	1.302	1.317	1.296
O4C4	1.188	1.199	1.280	1.284	1.319	1.301	1.315	1.296	1.190	1.202	1.194	1.205
H1N1	0.993	1.001	0.992	0.998								
H3N3	0.997	1.010	0.994	1.004					0.997	1.011	0.999	1.009
H5C5	1.070	1.070	1.071	1.070	1.071	1.071	1.074	1.075	1.071	1.071	1.073	1.076
H6C6	1.074	1.074	1.073	1.074	1.076	1.076	1.071	1.071	1.075	1.075	1.072	1.071
H1O2					0.944	0.954	0.945	0.958	0.946	0.958	0.945	0.959
H3O4					0.945	0.962	0.945	0.963				
Bond Angles												
N1C2N3	113.6	114.8	114.6	115.7	127.2	126.9	125.3	126.3	125.0	124.4	123.0	124.3
C2N3C4	127.8	126.5	125.6	124.9	116.0	116.9	111.7	112.2	123.2	123.0	110.9	116.4
N3C4C5	113.8	114.8	115.2	115.4	123.1	121.7	124.1	122.2	112.0	113.2	112.4	112.6
C2N1C6	123.2	122.7	123.3	122.8	115.5	115.3	118.2	116.6	115.3	115.5	115.6	116.1
C4C5C6	119.2	118.9	118.7	118.3	114.7	115.5	116.5	116.8	119.4	118.8	120.0	118.8
N1C6C5	122.3	122.3	121.9	122.1	123.5	123.7	106.1	107.2	125.1	125.1	118.4	115.5
N1C2O2	122.8	122.3	122.6	121.9	117.5	118.8	116.6	117.1	121.3	121.8	119.6	120.1
N3C2O2	123.6	122.9	122.7	122.4	115.3	114.3	118.0	116.6	113.6	113.8	115.7	115.4
N3C4O4	120.7	121.1	115.4	115.5	117.7	119.7	115.9	118.4	120.0	120.7	119.5	119.8
C5C4O4	125.5	124.1	118.3	116.9	119.3	118.6	120.0	119.4	127.9	126.1	128.1	127.5
C2N1H1	115.6	115.7	115.0	115.4								
C6N1H1	121.2	121.6	120.7	121.1								
C2N3H3	115.7	115.9	115.0	116.9					119.4	118.6	114.9	117.9
C4N3H3	116.5	117.6	119.1	118.2					117.4	118.4	112.6	117.9
C4C5H5	118.3	118.5	119.3	119.5	121.7	121.1	121.2	120.2	118.1	118.4	118.0	117.8
C6C5H5	122.5	122.7	122.0	122.2	123.6	123.5	121.9	121.9	122.6	122.8	121.9	121.7
N1C6H6	115.2	115.2	115.6	115.5	115.9	115.8	118.7	118.5	114.5	114.7	118.7	118.7
C5C6H6	122.5	122.5	122.5	122.3	120.6	120.5	121.2	121.7	120.4	120.2	122.5	123.6
C2O2H1					108.0	110.8	109.4	111.4	108.1	110.4	109.0	111.0
C4O4H3					108.4	113.0	108.3	113.0				
Dihedral Angles												
N3C2N1C6	0.0	0.7	7.0	−4.6	0.0	0.1	29.8	25.5	0.0	0.2	−28.4	5.2
C4N3C2N1	0.0	−1.0	0.8	−3.7	0.0	0.3	4.7	9.2	0.0	−0.3	52.1	−34.8
C5C4N3C2	0.0	0.8	−6.3	8.4	0.0	−0.6	−14.4	−16.2	0.0	0.2	−33.3	25.0
C6C5C4N3	0.0	−0.2	4.3	−5.1	0.0	0.4	−8.0	−8.9	0.0	−0.1	−0.3	8.1
C5C6N1C2	0.0	−0.3	−9.1	7.8	0.0	−0.4	−47.9	−47.2	0.0	−0.1	−11.3	29.6
N1C6C5C4	0.0	0.0	2.8	−2.4	0.0	0.2	37.4	39.8	0.0	0.0	24.6	−36.6
O2C2N1C6	180.0	179.2	−171. 7	173.9	180.0	179.9	−153. 0	−155.9	180.0	179.6	167.1	178.7
O4C4N3C2	180.0	179.2	137.1	−133. 0	180.0	179.4	166.6	163.4	180.0	179.8	144.9	−151.1
N3C2N1H1	180.0	179.9	175.5	−175. 5								
C5C4N3H3	180.0	179.0	166.1	−169. 0					180.0	179.2	−163. 8	173.6
H5C5C4N3	180.0	179.9	−174. 6	174.2	180.0	179.8	164.9	159.0	180.0	180.0	−177. 9	157.5
H6C6C5C4	180.0	179.9	−176. 0	175.8	180.0	180.0	176.8	179.1	180.0	179.9	162.5	160.3
H1O2C2N1					0.0	1.3	2.7	0.8	0.0	0.2	−8.1	1.3
H3O4C4N3					0.0	−1.8	−1.2	−3.3				

excitation; an increase in the hydrogen bond distance associated with the N1 site may be due to the nonplanarity of the molecule in the excited state. The geometry of the U-O2H1 tautomer in the $\pi\pi^*$ excited state is deformed mainly in the N3C2N1C6 region of the ring. Deformation is such that the N3C4C5C6 atoms are lying in a plane, while the C2N1 atoms are appreciably out of plane and slightly twisted along the perpendicular direction of the N1C2 bond. In going from the ground state to the $\pi\pi^*$ excited state, a large increase or decrease in the ring bond lengths is revealed (Table 4); the C5C6 bond length is increased by about 0.1 Å, while the N1C2 and N1C6 bond lengths are increased and decreased respectively by about 0.06 Å (Table 4). Among bond angles C2N3C4 is decreased by about 12° in the excited state. The hydrogen bond parameters for the hydrated U-O2H1 tautomer in the ground and excited states are shown in Figure 1d. This figure and the ring geometrical parameters shown in Table 4 suggest that hydration has little effect on the geometry of the molecule. The hydrogen bond distances do not change much as a result of the $\pi\pi^*$ excitation; however, the length of the hydrogen bond associated with the N1 site of the tautomer is increased in the excited state, which seems to be related to the nonplanarity of the molecule in the excited state (Table 4, Figure 1d). The geometrical parameters for the isolated and hydrated complexes of the U-O2H3 and U-O4H3 tautomers in the ground state are also shown in Figure 1e,f, respectively. The changes in geometrical parameters are only associated near the hydrogen bonding regions. Geometry optimizations of the lowest singlet $\pi\pi^*$ excited states for the U-O2H3 and U-O4H3 tautomers and their hydrated complexes and those for the hydrated complexes of the keto tautomer were not successful; in all cases, as the optimization proceeded, geometrical distortion and large twisting

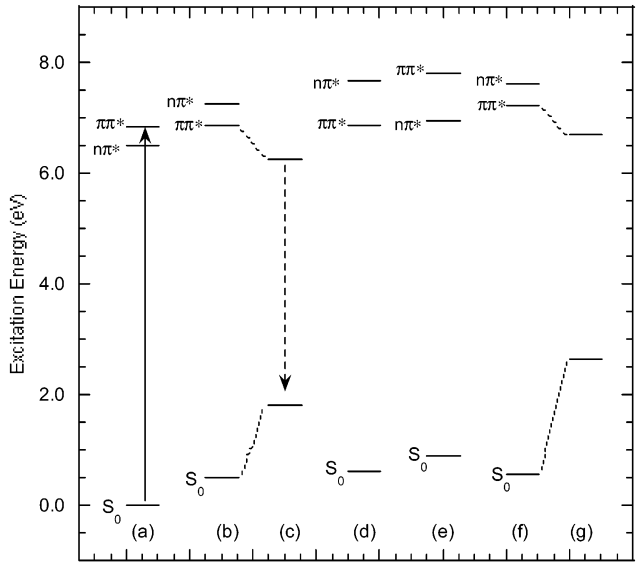

Figure 3. Energy level diagram of isolated uracil tautomers. Vertical states of uracil (keto), U-O2H1, U-O4H3, U-O2H3, and enol tautomers are shown in a, b, and d−f, respectively. The optimized state shown in c corresponds to the U-O2H1 tautomer, while g corresponds to the enol tautomer. The upward arrow corresponds to the absorption, while the downward arrow corresponds to the emission in the gas phase.

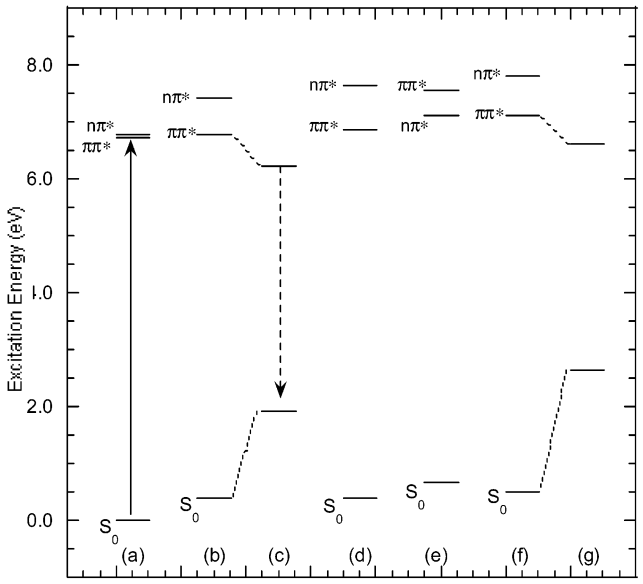

Figure 4. Energy level diagram of hydrated uracil tautomers. Vertical states of uracil (keto), U-O2H1, U-O4H3, U-O2H3, and enol tautomers are shown in a, b, and d−f, respectively. The optimized state shown in c corresponds to the U-O2H1 tautomer, while g corresponds to the enol tautomer. The upward arrow corresponds to the absorption, while the downward arrow corresponds to emission under the hydration.

of the C5C6 bond occurred. The excitation energy decreased to about 0.1 eV, and optimization aborted due to the lack of convergence. It should be noted that in an earlier geometry optimization study, uracil has been suggested to be dissociative around the C5C6 bond in the $\pi\pi^*$ excited state.[2] Similar results were also obtained in the case of the N1H tautomer of isocytosine in the $S_3(\pi\pi^*)$ excited state.[23a] Also in jet-cooled spectroscopic studies, a geometrical deformation of the $\pi\pi^*$ excited states of thymine and uracil has been suggested for the diffuseness in spectra of these compounds.[3]

3.5. Excited-State Phototautomerism. Low-lying vertical singlet $\pi\pi^*$ and $n\pi^*$ excitation energies of different tautomers of uracil in the gas phase and after hydration are presented in Table 2, while the corresponding energy level diagrams are shown in Figures 3 and 4. Energy level diagrams suggest that among the vertical lowest singlet $\pi\pi^*$ states of different tautomers, the state corresponding to the U-O2H1 and U-O4H3 tautomers are higher in energy by about 0.05 and 0.11 eV, respectively, than the corresponding state of uracil (keto), while those for the U-enol and U-O2H3 tautomers are appreciably higher (Figure 3). Under hydration, the lowest singlet vertical $\pi\pi^*$ excited state of the U-O2H1 and U-O4H3 tautomers is more close to the corresponding state of uracil (Figure 4). Therefore, there will be strong interaction among the lowest vertical singlet $\pi\pi^*$ states of the keto, U-O2H1, and U-O4H3 tautomers of uracil. Thus, under electronic excitation of uracil, an energy transfer from the lowest singlet $\pi\pi^*$ state of uracil to the corresponding state of U-O2H1 and U-O4H3 may take place. In other words, there is strong probability that uracil will phototautomerize to the U-O2H1 and U-O4H3 enol tautomers through energy transfer and necessary structural modifications. However, the rate of formation of these enol tautomers will also depend on the lifetime of the $S_1(\pi\pi^*)$ state of uracil (keto) and of the U-O2H1 and U-O4H3 tautomers. In the case of thymine, the lifetime of the keto form is found to be much smaller than the corresponding lifetime of enol tautomers.[12] It would lead to the formation of a small amount of the enol tautomers. It is also interesting to note that the scaled vertical first singlet $\pi\pi^*$ transition energy for the U-O2H1 and U-O4H3 tautomer are 4.58 and 4.51 eV, respectively (corresponding values of hydrated species are 4.61 and 4.62 eV, respectively), which are close to the 295 nm (4.20 eV) value. The excitation of a neutral aqueous solution of thymine by 295 nm gives rise to a fluorescence peak near 405 nm and is attributed to the emission from the enol tautomer.[12] The relaxed lowest singlet $\pi\pi^*$ excited state for the U-O2H1 tautomer in the gas phase and after hydration is also shown in energy level diagrams. It is clear that fluorescence due to the enol tautomers would originate from the relaxed lowest singlet $\pi\pi^*$ state of the U-O2H1 and U-O4H3 tautomers. The computed energy difference between the relaxed lowest singlet $\pi\pi^*$ excited of the hydrated U-O2H1 tautomer and the corresponding ground state lying vertically below it is 4.29 eV. The corresponding scaled value will be 3.09 eV, which is in good agreement with the 405 nm (3.06 eV) fluorescence observed in thymine after excitation at 295 nm.[12] Since we were not able to optimize the lowest singlet $\pi\pi^*$ excited state of the U-O4H3 tautomer, we cannot comment on it. The reason for the strong fluorescence peak for the enol tautomer of thymine compared to the normal tautomer may be due the longer excited-state lifetime of the former tautomer. A similar case has been observed between adenine and 2-aminopurine, where adenine has a very short lifetime with very poor fluorescence, while 2-aminopurine has a longer lifetime and very strong fluorescence.[23c,35]

4. Conclusions

The present study has led to the following important conclusions:

1. The absorption spectra is mainly dominated by the natural tautomeric form (keto) of uracil. The U-O2H1 and U-O4H3 enol forms of uracil would be formed via excited-state phototautomerization of the natural form of uracil. However, concentrations of these tautomers will be very small. These tautomers will yield red-shifted fluorescence compared to the natural fluorescence.

2. At a moderate alkaline pH in an aqueous medium, uracil would exist as a mixture of both neutral and monoanionic forms obtained by the deprotonation of the N1H site.

3. The ground-state geometries of uracil tautomers and their complexes are planar in the ground state; the corresponding geometry in the lowest singlet $\pi\pi^*$ state is highly nonplanar. Such distortions are localized mainly at the C5C6 bond of uracil.

4. The $n\pi^*$ excitation of hydrated uracil does not destroy the hydrogen bonding structures in contrast to the experimental observations of hydrated adenine.

Acknowledgment. Authors are thankful to NIH-RCMI Grant No. G1 2RR13459-21, NSF-CREST Grants No.9805465 & 9706268, and ONR Grant No. DAD 19-01-2-0014 for financial assistance. The authors are also thankful to the Mississippi Center for Supercomputing Research for the computational facilities.

References and Notes

(1) (a) Callis, P. R. *Annu. Rev. Phys. Chem.* **1983**, *34*, 329. (b) Eisinger, J.; Lamola, A. A. In *Excited State of Proteins and Nucleic Acids*; Steiner, R. F., Weinryb, I., Eds.; Plenum Press: New York, London, 1971. (c) Saenger, W. *Principles of Nucleic Structures*; Springer-Verlag: New York, 1984.

(2) Shukla, M. K.; Mishra, P. C. *Chem. Phys.* **1999**, *240*, 319.

(3) Brady, B. B.; Peteanu, L. A.; Levy, D. H. *Chem. Phys. Lett.* **1988**, *147*, 538.

(4) Chinsky, L.; Laigle, A.; Peticolas, L.; Turpin, P.-Y. *J. Chem. Phys.* **1982**, *76*, 1.

(5) (a) Leszczynski, J. In *Advances in Molecular Structure Research*; JAI Press: London, 2000; Vol. 6, p 209. (b) Sponer, J.; Hobza, P.; Leszczynski, J. In *Computational Molecular Biology, Theoretical and Computational Chemistry Book Series*; Leszczynski, J., Ed.; Elsevier: Amsterdam, 1999; Vol. 8, p 85. (c) Leszczynski, J. *J. Phys. Chem.* **1992**, *96*, 1649. (d) Leszczynski, J. *Int. J. Quantum Chem.: Quantum Biol. Symp.* **1991**, *18*, 9. (e) Petke, J. D.; Maggiora, G. M.; Christoffersen, R. E. *J. Phys. Chem.* **1992**, *96*, 6992. (f) Estrin, D. A.; Paglieri, L.; Corongiu, G. *J. Phys. Chem.* **1994**, *98*, 5653. (g) Kryachko, E. S.; Nguyen, M. T.; Zeegers-Huyskens, T. *J. Phys. Chem. A* **2001**, *105*, 1288.

(6) (a) Szczepaniak, K.; Person, W. B.; Leszczynski, J.; Kwiatkowski, J. S. *Pol. J. Chem.* **1998**, *72*, 402. (b) Drohat, A. C.; Stivers, T. J. *J. Am. Chem. Soc.* **2000**, *122*, 1840. (c) Schiedt, J.; Weinkauf, R.; Neumark, D. M.; Schlag, E. W. *Chem. Phys.* **1998**, *239*, 511. (d) Bell, A. F.; Hecht, L.; Barron, L. D. *J. Chem. Soc., Faraday Trans.* **1997**, *93*, 553. (e) Brown, R. D.; Godfrey, P. D.; McNaughton, D.; Pierlot, A. P. *J. Am. Chem. Soc.* **1988**, *110*, 2329. (f) Kulakowski, I.; Geller, M.; Lesyng, B.; Weirzchowski, K. L. *Biochim. Biophys. Acta* **1974**, *361*, 119. (g) Stewart, R. F. *Acta Crystallogr.* **1967**, *23*, 1102.

(7) Hauswirth, W. W.; Daniels, M. *Photochem. Photobiol.* **1971**, *13*, 157.

(8) Vigny, P.; Duquesne, M. *Photochem. Photobiol.* **1974**, *20*, 15.

(9) Suwaiyan, A.; Morsy, M. A.; Odah, K. A. *Chem. Phys. Lett.* **1995**, *237*, 349.

(10) Fujii, M.; Tamura, T.; Mikami, N.; Ito, M. *Chem. Phys. Lett.* **1986**, *126*, 583.

(11) Tsuchiya, Y.; Tamura, T.; Fujii, M.; Ito, M. *J. Phys. Chem.* **1988**, *92*, 1760.

(12) Morsy, M. A.; Al-Somali, A. M.; Suwaiyan, A. *J. Phys. Chem. B* **1999**, *103*, 11205.

(13) (a) Brandes, R.; Rupprecht, A.; Kearns, D. R. *J. Biophys.* **1989**, *56*, 683. (b) Wolf, B.; Hanlon, S. *Biochemistry* **1975**, *14*, 1661. (c) Franklin, R. E.; Gosling, R. G. *Nature* **1953**, *171*, 740.

(14) (a) Poltev, V. I.; Teplukhin, A. V.; Malenkov, G. G. *Int. J. Quantum Chem.* **1992**, *42*, 1499. (b) Kennard, O.; Hunter, W. N. *Angew. Chem., Int. Ed. Engl.* **1991**, *30*, 1254.

(15) (a) Gaigeot, M.-P.; Ghomi, M. *J. Phys. Chem. B* **2001**, *105*, 5007. (b) Mourik, T. van; Benoit, D. M.; Price, S. L.; Clary, D. C. *Phys. Chem. Chem. Phys.* **2000**, *2*, 1281. (c) Mourik, T. van. *Phys. Chem. Chem. Phys.* **2001**, *3*, 2886. (d) Bencivenni, L.; Ramondo, F.; Pieretti, A.; Sanna, N. *J. Chem. Soc., Perkin Trans.* **2000**, *2*, 1685.

(16) (a) Shishkin, O. V.; Gorb, L.; Leszczynski, J. *Int. J. Mol. Sci.* **2000**, *1*, 17. (b) Shishkin, O. V.; Gorb, L.; Hobza, P.; Leszczynski, J. *Int. J. Quantum Chem.* **2000**, *80*, 1116.

(17) Shukla, M. K.; Mishra, P. C. *Chem. Phys.* **1998**, *230*, 187.

(18) (a) Shukla, M. K.; Leszczynski, J. *J. Phys. Chem. A* **2002**, *106*, 1011. (b) Shukla, M. K.; Leszczynski, J. *J. Phys. Chem. A* **2002**, *106*, 4709.

(19) Korter, T. M.; Pratt, D. W.; Kupper, J. *J. Phys. Chem. A* **1998**, *102*, 7211.

(20) Kim, N. J.; Kang, H.; Jeong, G.; Kim, Y. S.; Lee, K. T.; Kim, S. K. *J. Phys. Chem. A* **2000**, *104*, 6552.

(21) Foresman, J. B.; Head-Gordon, M.; Pople, J. A.; Frisch, M. J. *J. Phys. Chem.* **1992**, *96*, 135.

(22) Frisch, M. J.; Trucks, G. W.; Schlegel, H. B.; Gill, P. M. W.; Johnson, B. G.; Robb, M. A.; Cheeseman, J. R.; Keith, T.; Petersson, G. A.; Montgomery, J. A.; Raghavachari, K.; Al-Laham, M. A.; Zakrzewski, V. G.; Ortiz, J. V.; Foresman, J. B.; Cioslowski, J.; Stefanov, B. B.; Nanayakkara, A.; Challacombe, M.; Peng, C. Y.; Ayala, P. Y.; Chen, W.; Wong, M. W.; Andres, J. L.; Replogle, E. S.; Gomperts, R.; Martin, R. L.; Fox, D. J.; Binkley, J. S.; Defrees, D. J.; Baker, J.; Stewart, J. P.; Head-Gordon, M.; Gonzalez, C.; Pople, J. A. *Gaussian 94*, Revision E.2; Gaussian, Inc.: Pittsburgh, PA, 1995.

(23) (a) Shukla, M. K.; Leszczynski, J. *Int. J. Quantum Chem.* **2000**, *77*, 240. (b) Mishra, S. K.; Shukla, M. K.; Mishra, P. C. *Spectrochim. Acta* **2000**, *56A*, 1355. (c) Broo, A. *J. Phys. Chem. A* **1998**, *102*, 526. (d) Shukla, M. K.; Mishra, S. K.; Kumar, A.; Mishra, P. C. *J. Comput. Chem.* **2000**, *21*, 826. (e) Holmen, A.; Broo, A.; Albinsson, B.; Norden, B. *J. Am. Chem. Soc.* **1997**, *119*, 12240. (f) Slater, L. S.; Callis, P. R. *J. Phys. Chem.* **1995**, *99*, 8572. (g) Fang, W.-H. *J. Chem. Phys.* **1999**, *111*, 5361.

(24) Scott, A.; Radom, L. *J. Phys. Chem.* **1996**, *100*, 16502.

(25) (a) Organero, J. A.; Diaz, A. V.; Moreno, M.; Santos, L.; Douhal, A. *J. Phys. Chem. A* **2001**, *105*, 7317. (b) Organero, J. A.; Moreno, M.; Santos, L.; Lluch, J. M.; Douhal, A. *J. Phys. Chem. A* **2000**, *104*, 8424. (c) Yamamoto, S.; Dierckxen, G. H. F.; Karelson, M. *Chem. Phys. Lett.* **2000**, *318*, 590. (d) Nishimura, Y.; Tsuji, T.; Sekiya, H. *J. Phys. Chem. A* **2001**, *105*, 7273.

(26) Chahinian, M.; Seba, H. B.; Ancian, B. *Chem. Phys. Lett.* **1998**, *285*, 337.

(27) (a) Sobolewski, A. L.; Domcke, W. *Chem. Phys. Lett.* **1999**, *300*, 533. (b) Sobolewski, A. L.; Domcke, W. *Chem. Phys.* **2000**, *259*, 181. (c) Sobolewski, A. L.; Domcke, W. *Chem. Phys. Lett.* **1999**, *315*, 293.

(28) Lorentzon, J.; Fulscher, M. P.; Roos, B. O. *J. Am. Chem. Soc.* **1995**, *117*, 9265.

(29) Backer, R. S.; Kogan, G. *Photochem. Photobiol.* **1980**, *31*, 5.

(30) (a) Voelter, W.; Records, R.; Bunnenburg, E.; Djerassi, C. *J. Am. Chem. Soc.* **1968**, *90*, 6113. (b) Brunner, W. C.; Maestre, M. F. *Biopolymers* **1975**, *14*, 555. (c) Sprecher, C. A.; Johnson, W. C., Jr. *Biopolymers* **1977**, *16*, 2243.

(31) Novros, J. S.; Clark, L. B. *J. Phys. Chem.* **1986**, *90*, 5666.

(32) (a) Clark, L. B.; Peschel, G. G.; Tinoco, I., Jr. *J. Phys. Chem.* **1965**, *69*, 3615. (b) Clark, L. B.; Tinoco, I., Jr. *J. Am. Chem. Soc.* **1965**, *87*, 11. (c) Voet, D.; Gratzer, W. B.; Cox, R. A.; Doty, P. *Biopolymers* **1963**, *1*, 193.

(33) (a) Matsuoks, Y.; Norden, B. *J. Phys. Chem.* **1982**, *86*, 1378. (b) Anex, B. G.; Fucaloro, A. F.; Durra-Ahmed, J. *J. Phys. Chem.* **1975**, *79*, 2636. (c) Eaton, W. A.; Lewis, T. P. *J. Chem. Phys.* **1970**, *53*, 2164. (d) Holmen, A.; Broo, A.; Albinsson, B. *J. Phys. Chem.* **1994**, *98*, 4998.

(34) Liptay, W. In *Excited States*; Lim, E. C., Ed.; Academic Press: New York, 1974; Vol. 1, p 129.

(35) (a) Nir, E.; Kleinermanns, K.; Grace, L.; de Vries, M. S. *J. Phys. Chem. A* **2001**, *105*, 5106. (b) Santhosh, C.; Mishra, P. C. *Spectrochim. Acta* **1991**, *47A*, 1685.